Radiative corrections in unpolarized elastic electron-deuteron scattering and deuteron charge radius puzzle

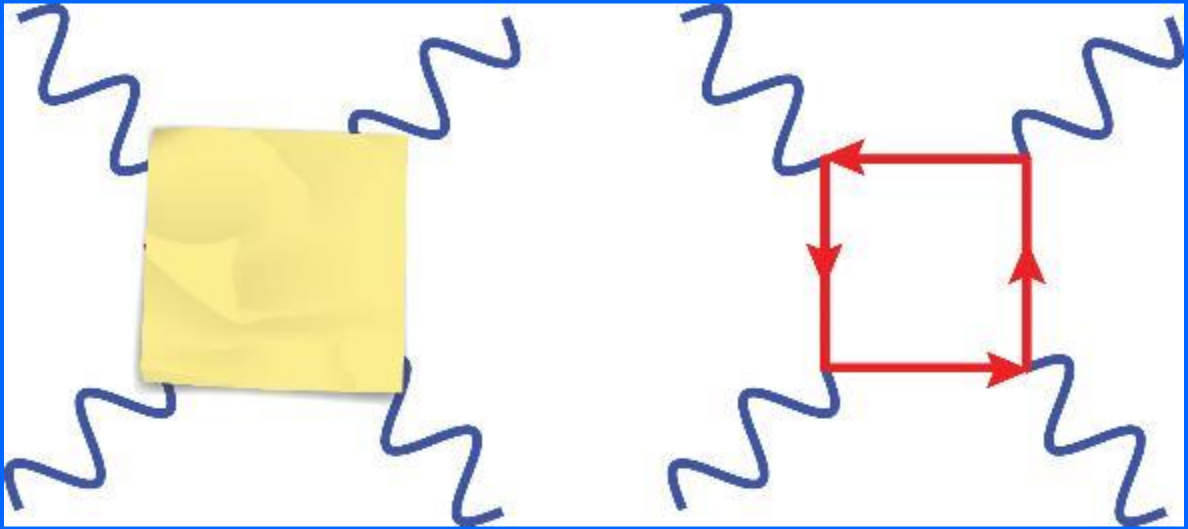

Vladimir Khachatryan

Hadronic Physics Group
Department of Physics, Indiana University

BNL Nuclear Theory Seminar

May 24 2024

Outline

1) Introduction

2) Unpolarized elastic e-d differential cross section and deuteron form-factor models

3) Observed cross section in e-d scattering

4) Numerical results for the proposed DRad experiment at Jefferson Lab

5) Proton and deuteron charge radius puzzles

6) Summary

1) Introduction

- Nucleons as building blocks of atomic nuclei
  - responsible for more than 99% of visible matter in the Universe
- The proton -- most stable hadron, a bound state of strong interactions driven by QCD
  - with quarks and gluons as fundamental degrees of freedom
- Root-mean-square (rms) electric/magnetic radius of the proton, $\sqrt{\langle r^2_{Ep,Mp} \rangle} \equiv r_p$
  - essential global quantity characterizing proton's size
  - related to proton's charge and magnetization distributions
- r_p as important input for bound-state QED calculations of hydrogen atom's energy levels
  - highly correlated with Rydberg constant, one of most precisely determined quantities
- Exact theoretical calculations of r_p from first principles being challenging
  - requires accurate knowledge of proton's internal structure at QCD non-perturbative regime
  - requires much better understanding how QCD works in low-energy region

1) Introduction

- Deuteron is of fundamental importance to nuclear physics, as the only bound two-nucleon system in nature, loosely bound with binding energy of 2.2 MeV

- Root-mean-square (rms) charge radius of the deuteron, $\sqrt{\langle r_{Ed}^2 \rangle} \equiv r_d$
  - essential global quantity characterizing deuteron's size
  - related to deuteron's charge distributions

Determine deuteron charge radius from elastic e-d structure function slope

$$r_d^2 = -6\left[\frac{dA(Q^2)}{dQ^2}\right]_{Q^2=0}$$

- Theoretical computations of deuteron form factors and rms radius
  - are independent of broad class of nucleon-nucleon potentials
  - depend mostly on neutron-proton scattering length and their binding energy

1) Introduction

- First measure elastic e-p and/or e-d cross sections

  Then determine form factors and eventually the radius

- JLab PRad collaboration proposed measurements of e-d elastic scattering to provide new result on deuteron charge radius r_d
  - with a planned experiment called DRad
  - with kinematic coverage of Q^2 from $1.8 \times 10^{-4}\ (\mathrm{GeV/c})^2$ to $5.3 \times 10^{-2}\ (\mathrm{GeV/c})^2$
  - with two electron beam energies of 1.1 GeV and 2.2 GeV

- DRad aiming at overall relative precision of 0.22% (or better) in determination of r_d

For e-p / e-d scattering cross section and proton/deuteron charge radius measurements, having reliable knowledge of radiative corrections with high precision is very important

1) Introduction

- Discuss mostly the results from epja2 paper

J. Zhou, V. Khachatryan, I. Akushevich, H. Gao, A. Ilyichev, et al.,
Lowest-order QED radiative corrections in unpolarized elastic electron-deuteron scattering beyond the ultra-relativistic limit for the proposed deuteron charge radius measurement at Jefferson laboratory
EPJ. A **59**, (2023) 256
(**epja2 made for proposed DRad experiment**)

A. Afanasev and A. Ilyichev,
EPJ. A **57**, (2021) 280

I. Akushevich, H. Gao, A. Ilyichev, and M. Meziane,
EPJ. A **51**, (2015) 1
(**epja1 made for finished PRad experiment**)

2) Unpolarized elastic cross section and form factors

- Take a glance at **e-p** scattering (Born approximation – one photon exchange)

$$e(k_1) + p(p_1) \rightarrow e'(k_2) + p(p_2)$$

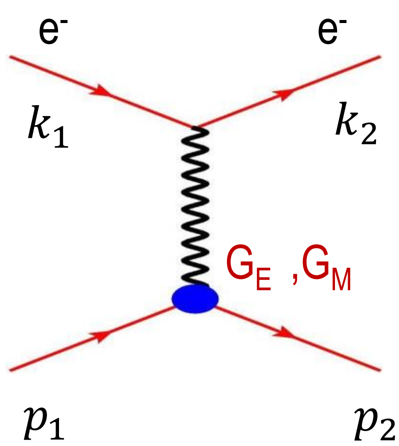

$$\frac{d\sigma}{d\Omega} = \left(\frac{d\sigma}{d\Omega}\right)_{\text{Mott}} \left(\frac{E'}{E}\right) \frac{1}{1+\tau} \left({G_E^p}^2(Q^2) + \frac{\tau}{\varepsilon} {G_M^p}^2(Q^2) \right)$$

$$Q^2 = 4EE' \sin^2\frac{\theta}{2} \qquad \tau = \frac{Q^2}{4M_p^2} \qquad \varepsilon = \left[1 + 2(1+\tau)\tan^2\frac{\theta}{2}\right]^{-1}$$

Mott cross section for structurless particle

$$\left(\frac{d\sigma}{d\Omega}\right)_{\text{Mott}} = \frac{\alpha^2\left[1-\beta^2\sin^2\frac{\theta}{2}\right]}{4k^2\sin^4\frac{\theta}{2}}$$

Taylor expansion of G_E at low Q^2

$$G_E^p(Q^2) = 1 - \frac{Q^2}{6}\langle r^2\rangle + \frac{Q^4}{120}\langle r^4\rangle + \ldots$$

Proton radius as a

derivative at low Q^2 limit

$$\sqrt{\langle r_{Ep}^2\rangle} = -\,6\,\frac{dG_E^p(Q^2)}{dQ^2}\bigg|_{Q^2=0}$$

- Electric, G_E, and magnetic, G_M, form factors can be extracted using the Rosenbluth separation method
  - G_E dominates at low Q^2

2) Unpolarized elastic cross section and form factors

- Matrix element of electromagnetic current operator of **e-d** scattering process given by

$$\mathcal{M} = ie^2 \bar{u}(k_2, \sigma_2)\gamma^\mu u(k_1, \sigma_1)\frac{1}{q^2}\langle p_2, \lambda_2 | j_\mu | p_1, \lambda_1 \rangle$$

- Deuteron electromagnetic current operator given by

$$\begin{aligned}\langle p_2, \lambda_2 | j_\mu | p_1, \lambda_1 \rangle &\equiv G^\mu_{\lambda_2,\lambda_1}(p_2, p_1)\\
&= -\Big\{ G_1^d(q^2)\left(\xi^*_{\lambda_2}(p_2)\cdot\xi_{\lambda_1}(p_1)\right)(p_2+p_1)^\mu\\
&\quad + G_2^d(q^2)\Big[\xi^\mu_{\lambda_1}(p_1)\left(\xi^*_{\lambda_2}(p_2)\cdot q\right)\\
&\quad - \xi^{\mu *}_{\lambda_2}(p_2)\left(\xi_{\lambda_1}(p_1)\cdot q\right)\Big]\\
&\quad - G_3^d(q^2)\frac{1}{2M_d^2}\left(\xi^*_{\lambda_2}(p_2)\cdot q\right)\left(\xi_{\lambda_1}(p_1)\cdot q\right)\\
&\quad \times (p_2+p_1)^\mu \Big\},\end{aligned}$$

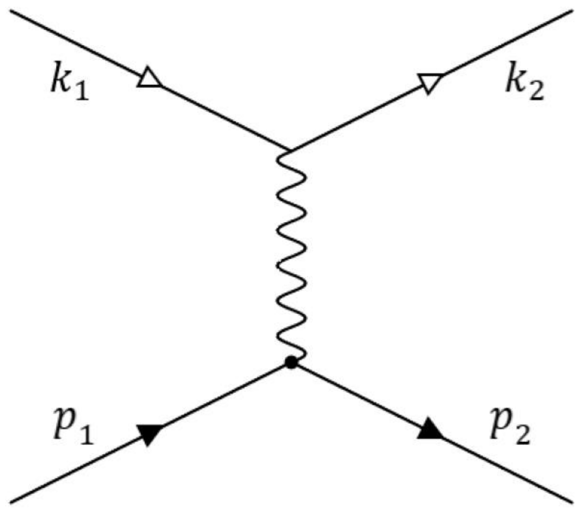

Feynman diagram contributing to Born cross section for elastic e-d scattering

$\sigma_{1,2}$ and $\lambda_{1,2}$ are helicities of incoming/outgoing lepton and incoming/outgoing deuteron respectively

ξ_{λ_1} and ξ_{λ_2} are polarization four vectors of initial and final deuteron states

2) Unpolarized elastic cross section and form factors

- $Q^2 = -q^2$ dependent form factors G_i^d related to combinations of three form factors:

  charge monopole G_C^d, magnetic dipole G_M^d, and charge quadrupole G_Q^d

$$G_C^d(Q^2) = G_1^d(Q^2) + \frac{2}{3}\,\eta\, G_Q^d(Q^2),$$
$$G_M^d(Q^2) = G_2^d(Q^2),$$
$$G_Q^d(Q^2) = G_1^d(Q^2) - G_2^d(Q^2) + (1+\eta)\, G_3^d(Q^2)$$

with additional relations given by

$$G_C^d(0) = 1, \qquad \frac{G_M^d(0)}{\mu_M^d} = 1, \qquad \frac{G_Q^d(0)}{\mu_Q^d} = 1 \qquad\qquad \eta \equiv Q^2/4M_d^2$$

μ_d -- deuteron magnetic dipole moment (in units of $e/2M_d$)
Q_d -- deuteron electric quadrupole moment (in units of e/M_d^2)

2) Unpolarized elastic cross section and form factors

- Now consider unpolarized elastic e+d scattering (Born approximation)

$$e(k_1) + d(p_1) \to e'(k_2) + d(p_2)$$

- Cross section represented by

$$\frac{d\sigma^B}{d\theta_e}(E_1,\theta_e) = \sigma_{NS}(E_1,\theta_e) \times \left(A_d(Q^2) + B_d(Q^2)\tan^2\left(\frac{\theta_e}{2}\right)\right)$$

Mott cross section for structurless particle

$$\boxed{\begin{aligned}\sigma_{NS}(E_1,\theta_e) &\equiv \left(\frac{d\sigma}{d\theta_e}(E_1,\theta_e)\right)_{\text{Mott}} \\ &= 2\pi\,\frac{4\alpha^2 E_2^2}{Q^4}\frac{E_2}{E_1}\left(1-\sin^2\left(\frac{\theta_e}{2}\right)\right)\sin(\theta_e)\end{aligned}}$$

with deuteron electromagnetic structure functions

$$A_d(Q^2) = \left(G_C^d(Q^2)\right)^2 + \frac{2}{3}\eta\left(G_M^d(Q^2)\right)^2 + \frac{8}{9}\eta^2\left(G_Q^d(Q^2)\right)^2,$$

$$B_d(Q^2) = \frac{4}{3}\eta(1+\eta)\left(G_M^d(Q^2)\right)^2,$$

Relation of scattered electron energy and incoming (beam) electron energy

$$\boxed{E_2 = \frac{E_1}{1+(2E_1/M_d)\sin^2(\theta_l/2)}}$$

2) Unpolarized elastic cross section and form factors

- Use current deuteron four form-factor models: see **epja2** for more details
  - **Abbott1, Abbott2, Parker, SOG (Sum-of-Gaussian)**

- **Abbott1** model:

$$G_X^d(Q^2) = G_X^d(0) \times \left[1 - \left(\frac{Q}{Q_X^0}\right)^2\right] \times \left[1 + \sum_{i=1}^{5} a_{Xi}\, Q^{2i}\right]^{-1}$$

with $X = C$, M, and Q

- Three form factors G_C^d, G_M^d, G_Q^d have generic form

Three $G_X^d(0)$ numbers are normalizing factors fixed by deuteron static moments

Free parameters Q_X^d and a_{Xi} shown on the right

$$Q_C^0 = 4.21\ \mathrm{fm}^{-1};$$

$$a_{Ci} = 6.740 \cdot 10^{-1},\ 2.246 \cdot 10^{-2},\ 9.806 \cdot 10^{-3},\ -2.709 \cdot 10^{-4},\ 3.793 \cdot 10^{-6};\ Q_M^0 = 7.37\ \mathrm{fm}^{-1};$$

$$a_{Mi} = 5.804 \cdot 10^{-1},\ 8.701 \cdot 10^{-2},\ -3.624 \cdot 10^{-3},\ 3.448 \cdot 10^{-4},\ -2.818 \cdot 10^{-6};\ Q_Q^0 = 8.10\ \mathrm{fm}^{-1};$$

$$a_{Qi} = 8.796 \cdot 10^{-1},\ -5.656 \cdot 10^{-2},\ 1.933 \cdot 10^{-2},$$

2) Unpolarized elastic cross section and form factors

- Second parametrization called **Abbott2** given by the following set of expressions

$$G_C^d(Q^2) = \frac{(G(Q^2))^2}{(2\eta+1)}\left[\left(1-\frac{2}{3}\eta\right)g_{00}^{+} + \frac{8}{3}\sqrt{2\eta}\,g_{+0}^{+} + \frac{2}{3}(2\eta-1)\,g_{+-}^{+}\right],$$

$$G_M^d(Q^2) = \frac{(G(Q^2))^2}{(2\eta+1)}\left[2g_{00}^{+} + \frac{2(2\eta-1)}{\sqrt{2\eta}}\,g_{+0}^{+} - 2g_{+-}^{+}\right]$$

$$G_Q^d(Q^2) = \frac{(G(Q^2))^2}{(2\eta+1)}\left[-g_{00}^{+} + \sqrt{\frac{2}{\eta}}\,g_{+0}^{+} - \frac{\eta+1}{\eta}g_{+-}^{+}\right]$$

with dipole form factor $G(Q^2)$

$$G(Q^2) = \left(1+\frac{Q^2}{\delta^2}\right)^{-2}$$

δ – parameter of the nucleon mass order

$$g_{00}^{+} = \sum_{i=1}^{n}\frac{a_i}{\alpha_i^2+Q^2}, \quad g_{+0}^{+} = Q\sum_{i=1}^{n}\frac{b_i}{\beta_i^2+Q^2},$$

$$g_{+-}^{+} = Q^2\sum_{i=1}^{n}\frac{c_i}{\gamma_i^2+Q^2},$$

The sets $\{a_i, \alpha_i^2\}, \{b_i, \beta_i^2\}, \{c_i, \gamma_i^2\}$, are fitting parameters

For Parker and SOG form-factor models see Appendix A of **epja2** for more details

3) Observed cross section

- Consider the process of bremsstrahlung with radiated photon

$$e(k_1) + d(p_1) \to e'(k_2) + d(p_2) + \gamma(k)$$

- Cross section of that process is

$$\mathrm{d}\sigma_R = \frac{1}{2\sqrt{\lambda_S}} \mathcal{M}_R^2 \, \mathrm{d}\Gamma_3$$

where

$$\lambda_S = S^2 - 4m_e^2 M_d^2 \qquad S = 2k_1 \cdot p_1 = 2E_1 \cdot M_d$$

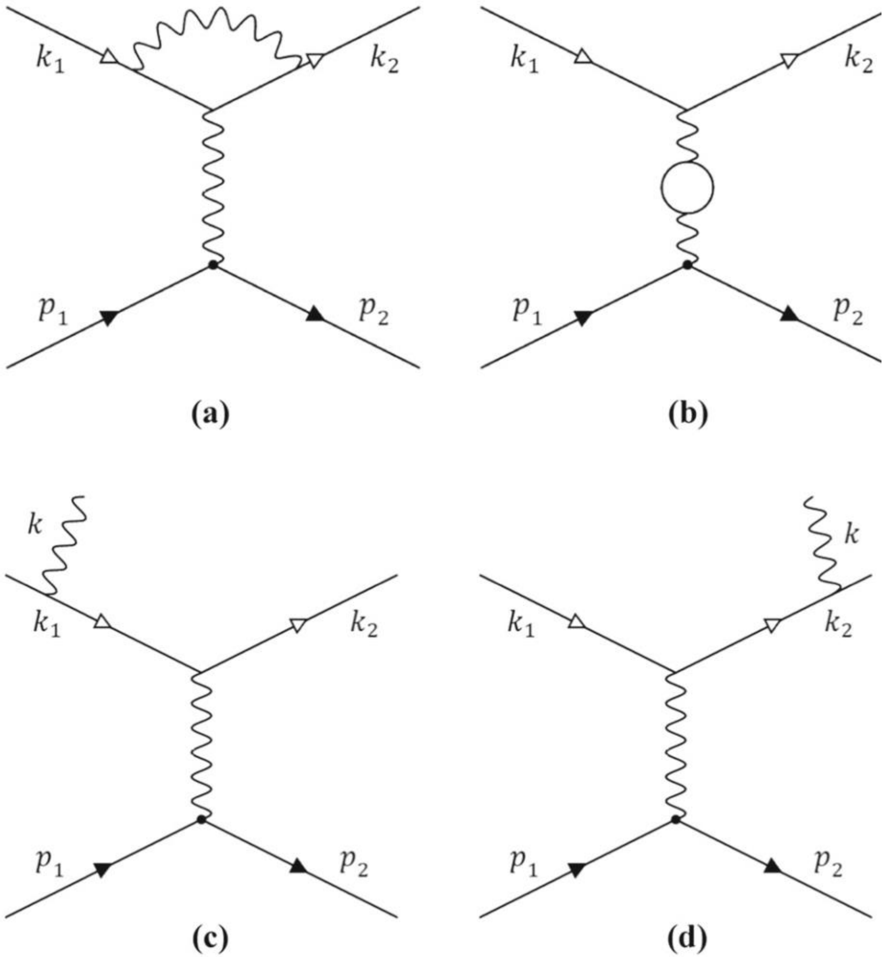

Feynman diagrams describing lowest-order QED RC contributions to unpolarized elastic e-d scattering cross section

(a) vertex correction; (**b)** vacuum polarization; **(c)**, (**d)** electron-leg bremsstrahlung

3) Observed cross section

- Phase-space element $d\Gamma_3$ is described in terms of three additional quantities called "photonic variables"

$$\upsilon = (p_1 + k_1 - k_2)^2 - M_d^2, \qquad \tau = \frac{k \cdot q}{k \cdot p_1}, \qquad \phi_k$$

in which υ is inelasticity, φ_k is azimuthal angle between $(\mathbf{k_1}, \mathbf{k_2})$ and $(\mathbf{k}, \mathbf{q})$ planes in the rest frame ($\mathbf{p_1} = 0$)

- Real hard photon contribution to observed cross section can be considerably reduced by applying cut on inelasticity quantity

- Two inelasticity cut-off values, υ_{cut} and $\upsilon_{\min}$, are considered in our calculations where we have $\upsilon_{\min} \leq \upsilon_{\text{cut}} \leq \upsilon_q^{\max}$

$$\upsilon_q^{\max} = S - 2m_e\left(\sqrt{S + m_e^2 + M_d^2} - m_e\right)$$

Also, $Q^2 \leftrightarrow \theta_e$ transformation reads as

$$Q^2 = 2E_1E_2 - 2m_e^2 - 2\sqrt{E_1^2 - m_e^2}\sqrt{E_2^2 - m_e^2}\cos(\theta_e)$$

3) Observed cross section

- Total cross section has the following components

see Section 3.2 of **epja2** for more details

• RC term δ_{VR}	Sum of all infrared divergent terms
• RC term $\delta^{l}_{\mathrm{vac}}$	Leptonic vacuum polarization correction to electric Dirac form factor of electromagnetic vertex
• RC term $\delta^{h}_{\mathrm{vac}}$	Hadronic vacuum polarization correction to electric Dirac form factor of the electromagnetic vertex
• RC term δ_{inf}	Approximate higher-order RC contribution by exponentiation procedure
• Cross-section terms $\mathrm{d}\sigma^{\mathrm{AMM}}/\mathrm{d}Q^2$ and $\mathrm{d}\sigma^{\mathrm{AMM}}/\mathrm{d}\theta_e$	Anomalous magnetic moment's contribution to cross section
• Cross-section terms $\mathrm{d}\sigma^{F}_{R}/\mathrm{d}Q^2$ and $\mathrm{d}\sigma^{F}_{R}/\mathrm{d}\theta_e$	Infrared-free contribution to cross section

3) Observed cross section

Transformation Jacobian of Born cross section

$$\frac{\mathrm{d}\sigma^B}{\mathrm{d}Q^2} = -\frac{1}{j_\theta \sin(\theta_e)} \frac{\mathrm{d}\sigma^B}{\mathrm{d}\theta_e} \qquad j_\theta = -\frac{\sqrt{\lambda_S}\,\lambda_X^{3/2}}{2M_d^2\left(SX - 2m_e^2\left(Q^2 + 2M_d^2\right)\right)}$$

Bardin-Shumeiko method for infrared divergence cancellation

- Use the following transformation, to extract infrared divergence

$$\mathrm{d}\sigma_R = \left(\mathrm{d}\sigma_R - \mathrm{d}\sigma_R^{IR}\right) + \mathrm{d}\sigma_R^{IR} = \mathrm{d}\sigma_R^F + \mathrm{d}\sigma_R^{IR}$$

σ_R^F and σ_R^{IR} being infrared divergence-free and divergence-dependent contributions of cross section

σ_R^F becomes finite at $k \to 0$

- Obtain σ_R^{IR} before integration over the variable φ_k

$$\frac{\mathrm{d}\sigma_R^{IR}}{\mathrm{d}Q^2} = \frac{1}{R}\lim_{R\to 0}\left[R\,\frac{\mathrm{d}\sigma_R}{\mathrm{d}Q^2}\right] = -\frac{\alpha}{\pi^2}\frac{F_{IR}}{R^2}\frac{\mathrm{d}^3k}{k_0}\frac{\mathrm{d}\sigma^B}{\mathrm{d}Q^2} \qquad R = 2k\cdot p_1 = \frac{\upsilon}{1+\tau}$$

- $d\sigma_R^{IR}/dQ^2$ needs to be separated into soft δ_S and hard δ_H parts by splitting integration region over inelasticity υ
  - do it by introducing infinitesimal photon energy $\lambda \to 0$ defined in system $\mathbf{p_1} + \mathbf{q} = 0$ system

3) Observed cross section

- Summation of all infrared divergent terms itself is free of any infrared divergence
- To cancel infrared divergences, include also leptonic vertex correction, δ_{vert}
- Components with infinitesimal photon energy canceling out explicitly in summation

$$\begin{aligned}\delta_{VR}(Q^2) &= \delta_{IR} + \delta_{\text{vert}} \\ &= 2\left(\left(Q^2 + 2m_e^2\right) L_m - 1\right) \ln\left(\frac{v_{\text{cut}}}{m_e M_d}\right) \\ &\quad + \frac{1}{2}\left(S L_S + X L_X\right) + S_\phi\left(k_1, k_2, p_2\right) \\ &\quad + \left(\frac{3}{2} Q^2 + 4m_e^2\right) L_m - 2 - \frac{(Q^2 + 2m_e^2)}{\sqrt{\lambda_m}} \\ &\quad \times \left(\frac{1}{2}\lambda_m L_m^2 + 2\,\text{Li}_2\left(\frac{2\sqrt{\lambda_m}}{Q^2 + \sqrt{\lambda_m}}\right) - \frac{\pi^2}{2}\right)\end{aligned}$$

$$L_m = \frac{1}{\sqrt{\lambda_m}} \ln\left(\frac{\sqrt{\lambda_m} + Q^2}{\sqrt{\lambda_m} - Q^2}\right) \qquad L_X = \frac{1}{\sqrt{\lambda_X}} \ln\left(\frac{X + \sqrt{\lambda_X}}{X - \sqrt{\lambda_X}}\right)$$

$$L_S = \frac{1}{\sqrt{\lambda_S}} \ln\left(\frac{S + \sqrt{\lambda_S}}{S - \sqrt{\lambda_S}}\right) \qquad \lambda_X = X^2 - 4m_e^2 M_d^2$$

$$\begin{aligned}S_\phi(k_1, k_2, p_2) = \frac{Q^2 + 2m_e^2}{\sqrt{\lambda_m}} \Bigg(&\frac{1}{4}\lambda_X L_X^2 - \frac{1}{4}\lambda_S L_S^2 \\ &+ \text{Li}_2\left[1 - \frac{(X + \sqrt{\lambda_X})\,T}{8m_e^2 M_d^2}\right] \\ &+ \text{Li}_2\left[1 - \frac{T}{2(X + \sqrt{\lambda_X})}\right] \\ &- \text{Li}_2\left[1 - \frac{Q^2(S + \sqrt{\lambda_S})\,T}{2M_d^2(Q^2 + \sqrt{\lambda_m})^2}\right] \\ &- \text{Li}_2\left[1 - \frac{2m_e^2 Q^2 T}{(Q^2 + \sqrt{\lambda_m})^2 (S + \sqrt{\lambda_S})}\right]\Bigg)\end{aligned}$$

$$X = S - Q^2$$

$$T = \frac{\left(Q^2 + \sqrt{\lambda_m}\right)\left(S_p - \sqrt{\lambda_m}\right)}{\sqrt{\lambda_m}} \qquad \text{Li}_2(x) = -\int_0^x \frac{\ln|1 - y|}{y}\,dy$$

$$S_p = S + X = 2S - Q^2$$

3) Observed cross section

- Leptonic vacuum polarization correction originated by *e*, *μ*, and *τ* charged leptons

$$\delta^{l}_{\text{vac}}(Q^2) = \sum_{i=e,\mu,\tau} \delta^{l,i}_{\text{vac}} = \sum_{i=e,\mu,\tau} \left(\frac{2}{3}\left(Q^2 + 2m_i^2\right) L^i_m - \frac{10}{9} + \frac{8m_i^2}{3Q^2}\left(1 - 2m_i^2 L^i_m\right) \right)$$

$$L^i_m = \frac{1}{\sqrt{\lambda^i_m}} \ln\left(\frac{\sqrt{\lambda^i_m} + Q^2}{\sqrt{\lambda^i_m} - Q^2} \right)$$

$$\lambda^i_m = Q^2\left(Q^2 + 4m_i^2\right)$$

- Hadronic vacuum polarization correction by hadrons
  - taken as a fit to experimental cross section data for *e^+e^- annihilation to hadrons*

$$\delta^{h}_{\text{vac}}(Q^2) = -\frac{2\pi}{\alpha}\left[\varDelta + \varXi \log(1 + \varSigma\, Q^2)\right]$$

$$|t| = Q^2$$

$\lvert t\rvert$, $(\mathrm{GeV}/c)^2$	$\varDelta$	$\varXi$	$\varSigma$
$0-1$	-1.345×10^{-9}	-2.302×10^{-3}	4.091

3) Observed cross section

➢ As first approximation, contributions of higher-order RCs to be considered by so-called exponentiation procedure

- given by term $e^{(\alpha/\pi)\delta_{\inf}}$

$$\boxed{\delta_{\inf}(Q^2) = \left(Q_m^2 L_m - 1\right) \ln\left(\frac{\upsilon_{\mathrm{cut}}^2}{S(S-Q^2)}\right)}$$

- to simply account for multiphoton radiation's contribution at $Q^2 \to 0$

➢ Anomalous magnetic moment's contribution to cross section stemming from leptonic vertex correction

$$\frac{\mathrm{d}\sigma^{\mathrm{AMM}}}{\mathrm{d}Q^2} = \frac{\alpha^3 m_e^2 L_m}{2M_d^2 Q^2 \lambda_S} \times \left(12 M_d^2\, W_{1d}(Q^2) - \left(Q^2 + 4M_d^2\right) W_{2d}(Q^2)\right)$$

$$\frac{\mathrm{d}\sigma^{\mathrm{AMM}}}{\mathrm{d}Q^2} = -\frac{1}{j_\theta \sin(\theta_e)} \frac{\mathrm{d}\sigma^{\mathrm{AMM}}}{\mathrm{d}\theta_e}$$

$$W_{1d}(Q^2) = 2M_d^2\, B_d(Q^2)$$

$$W_{2d}(Q^2) = 4M_d^2\, A_d(Q^2)$$

$$\frac{\mathrm{d}\sigma^{B}}{\mathrm{d}Q^2}\left(E_1, Q^2\right) = \frac{2\pi\alpha^2}{\lambda_S\, Q^4}\left(\theta_B^1\, W_{1d}(Q^2) + \theta_B^2\, W_{2d}(Q^2)\right)$$

$$\theta_B^1 = Q^2 - 2m_e^2 \qquad \theta_B^2 = \frac{SX - M_d^2 Q^2}{2M_d^2}$$

3) Observed cross section

- Infrared-free contribution σ_R^F -- last ingredient of unpolarized e-d elastic scattering cross section

$$d\sigma_R = \frac{1}{2\sqrt{\lambda_S}} \mathcal{M}_R^2 \, d\Gamma_3$$

- Matrix element represented as

$$\mathcal{M}_R^2 = \frac{(4\pi\alpha)^3}{\tilde{Q}^4} \times L_R^{\mu\nu} \left(\tilde{w}^1_{\mu\nu} \, W_{1d}(\tilde{Q}^2) + \tilde{w}^2_{\mu\nu} \, W_{2d}(\tilde{Q}^2) \right)$$

- Symbol "tilde" meaning Q^2 defined by shifted argument

$$\tilde{Q}^2 = -(q-k)^2 = Q^2 + R\tau$$

- Use three "photonic" variables on slide 14

- Integrate σ_R over φ_k analytically, then over τ variable
- After infrared divergence extraction, integrate over υ

$$\frac{d\sigma_R^F}{dQ^2} = -\frac{\alpha^3}{2\lambda_S} \int_0^{\upsilon_{\text{cut}}} d\upsilon \sum_{i=1}^{2} \Bigg[4 \, \frac{J_0 \, \theta_B^i \, W_{id}(Q^2)}{\upsilon \, Q^4} + \int_{\tau_q^{\min}}^{\tau_q^{\max}} \frac{d\tau}{(1+\tau)\,\tilde{Q}^4} \sum_{j=1}^{k_i} W_{id}(\tilde{Q}^2) \, R^{j-2} \, \theta_{ij}(\upsilon, \tau, Q^2) \Bigg]$$

$$\tau_q^{\max,\min} = \frac{\upsilon + Q^2 \pm \sqrt{\lambda_q}}{2M_d^2}$$

$$\lambda_q = \left(\upsilon + Q^2\right)^2 + 4M_d^2 Q^2$$

$$J_0 = 2\left(\left(Q^2 + 2m_e^2\right) L_m - 1\right)$$

3) Observed cross section

- Same cross-section term as a function of scattering angle to be given by

$$\frac{d\sigma_R^F}{d\theta_e} = \sin(\theta_e)\left(\frac{\alpha^3}{2\lambda_S}\right) \times \int_0^{\upsilon_{\text{cut}}} d\upsilon \sum_{i=1}^{2}\Bigg[4\, j_\theta\, \frac{J_0\, \theta_B^i\, W_{id}(Q^2)}{\upsilon\, Q^4}$$

$$+ J_\theta(\upsilon) \int_{\tau_\theta^{\min}}^{\tau_\theta^{\max}} \frac{d\tau}{(1+\tau)\,\tilde{Q}^4} \times \sum_{j=1}^{k_i} W_{id}(\tilde{Q}^2)\, R^{j-2}\, \theta_{ij}\Big(\upsilon, \tau, Q_R^2(\upsilon)\Big)\Bigg]$$

$$\tau_\theta^{\max,\min} = \frac{\upsilon + Q_R^2(\upsilon) \pm \sqrt{\lambda_\upsilon}}{2M_d^2} \qquad \lambda_\upsilon = \Big(\upsilon + Q_R^2(\upsilon)\Big)^2 + 4M_d^2 Q_R^2(\upsilon)$$

$$Q_R^2(\upsilon) = \frac{1}{\left(S + 2M_d^2\right)^2 - \lambda_S \cos^2(\theta_e)}$$

$$\times\bigg(\Big(S+2M_d^2\Big)\,(\lambda_S - \upsilon S) - \lambda_S (S-\upsilon)\cos^2(\theta_e) - 2M_d\sqrt{\lambda_S}\,\sqrt{\mathcal{D}}\cos(\theta_e)\bigg)$$

$$\mathcal{D} = M_d^2\,(\lambda_S + \upsilon(\upsilon - 2S)) - m_e^2\left(\lambda_S \sin^2(\theta_e) + 4\upsilon M_d^2\right)$$

3) Observed cross section

Observed (total) cross section
as functions of four-momentum
transfer squared Q^2
and
scattering angle θ_e

for unpolarized elastic
e-d scattering

beyond ultrarelativistic
approximation ($m_e \ll M_d$)

including lowest-order
RC contributions

is expressed as follows

$$\frac{d\sigma^{\rm obs}}{dQ^2} = \left[1 + \frac{\alpha}{\pi}\left(\delta_{VR}(Q^2) + \delta^l_{\rm vac}(Q^2) + \delta^h_{\rm vac}(Q^2) - \delta_{\rm inf}(Q^2)\right)\right] \times \left[e^{(\alpha/\pi)\,\delta_{\rm inf}(Q^2)}\right] \frac{d\sigma^B}{dQ^2} + \frac{d\sigma^{\rm AMM}}{dQ^2} + \frac{d\sigma^F_R}{dQ^2}$$

$$\frac{d\sigma^{\rm obs}}{d\theta_e} = \left[1 + \frac{\alpha}{\pi}\left(\delta_{VR}(\theta_e) + \delta^l_{\rm vac}(\theta_e) + \delta^h_{\rm vac}(\theta_e) - \delta_{\rm inf}(\theta_e)\right)\right] \times \left[e^{(\alpha/\pi)\,\delta_{\rm inf}(\theta_e)}\right] \frac{d\sigma^B}{d\theta_e} + \frac{d\sigma^{\rm AMM}}{d\theta_e} + \frac{d\sigma^F_R}{d\theta_e}$$

3) Observed cross section

- Mentioning Møller scattering (see **epja1**)

$$e(k_1) + e(p_1) \rightarrow e'(k_2) + e'(p_2)$$

- During PRad experiment, luminosity monitored by simultaneously measuring the Møller scattering process
- Absolute e+p elastic scattering cross section is normalized to that of Møller scattering to cancel out luminosity
- Same will happen for DRad experiment
- Møller process contributes to systematic uncertainties for measured radius

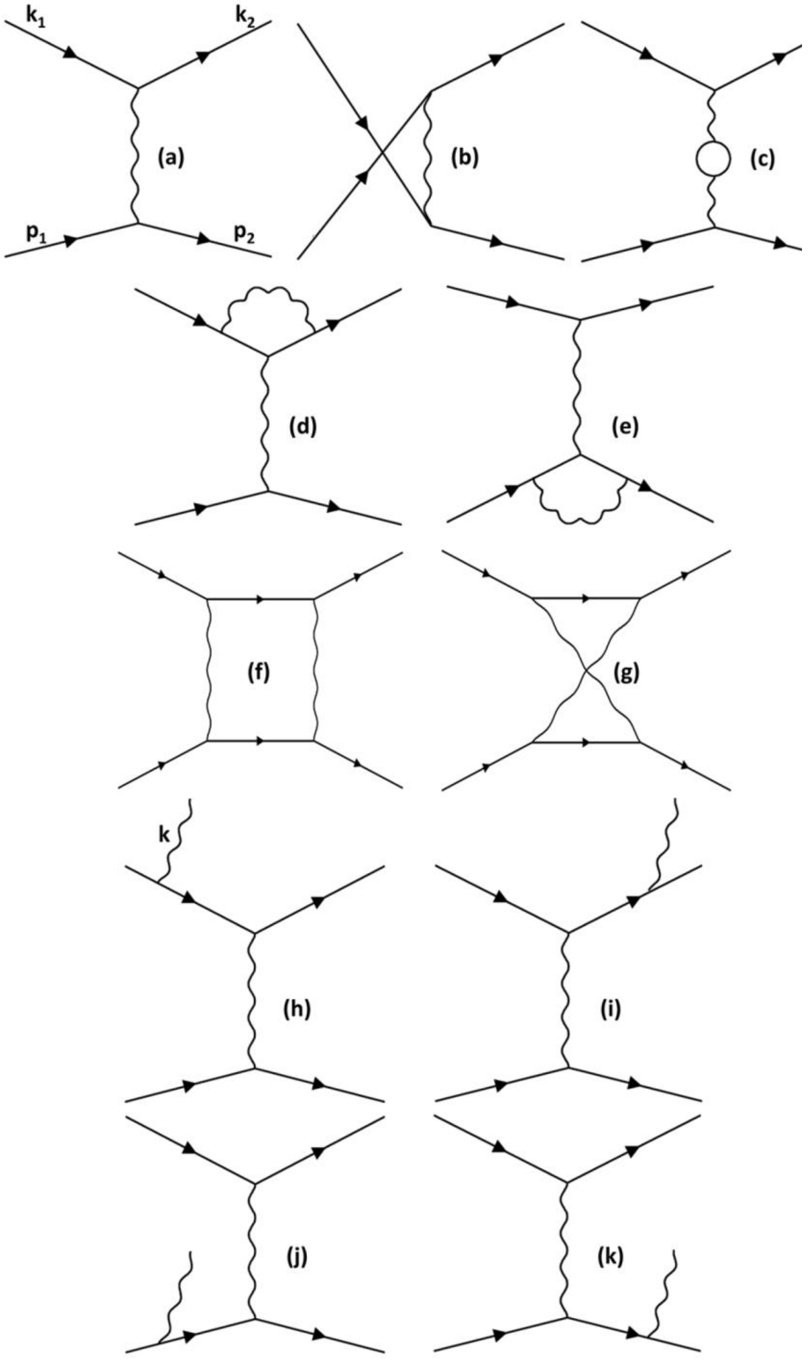

Feynman diagrams contributing to
Born (a)-(b) and RC cross sections
for Møller scattering:
(c)-(e) Vacuum polarization and vertex correction
(f)-(g) Box contributions (h)-(k) Bremsstrahlung

4) Numerical results

- As mentioned on slide 14, two inelasticity cut-off values, v_{cut} and v_{min}, are considered in our calculations

- v_{cut} being experimental quantity
  - can be considered as upper limit of Bremsstrahlung integration
  - and inelasticity cut-off value for performing calculations in the range of interest

- v_{min} corresponds to minimal energy of a radiative photon that can be detected

- Quantify soft part of lowest-order radiative corrections as a function of scattering angle and four-momentum transfer squared

$$\delta_{ed} = \left(\frac{\mathrm{d}\sigma^{\text{soft}}}{\mathrm{d}\theta_e} \middle/ \frac{\mathrm{d}\sigma^{B}}{\mathrm{d}\theta_e} \right) - 1 \qquad \delta_{ed} = \left(\frac{\mathrm{d}\sigma^{\text{soft}}}{\mathrm{d}Q^2} \middle/ \frac{\mathrm{d}\sigma^{B}}{\mathrm{d}Q^2} \right) - 1$$

- $\boldsymbol{\delta_{ed}}$ defined as relative difference between soft and Born differential cross sections

4) Numerical results

Unpolarized elastic **e-d** scattering
Observed cross section
as a function of θ_e **(top panel)**
and
as a function of Q^2 **(bottom panel)**
at
E_1 = 1.1 GeV (solid lines),
E_1 = 2.2 GeV (dashed lines)

Solid lines describe Born cross section

Dot-dashed lines describe cross sections with soft part of radiative corrections

Abbott1 form-factor model used in calculations

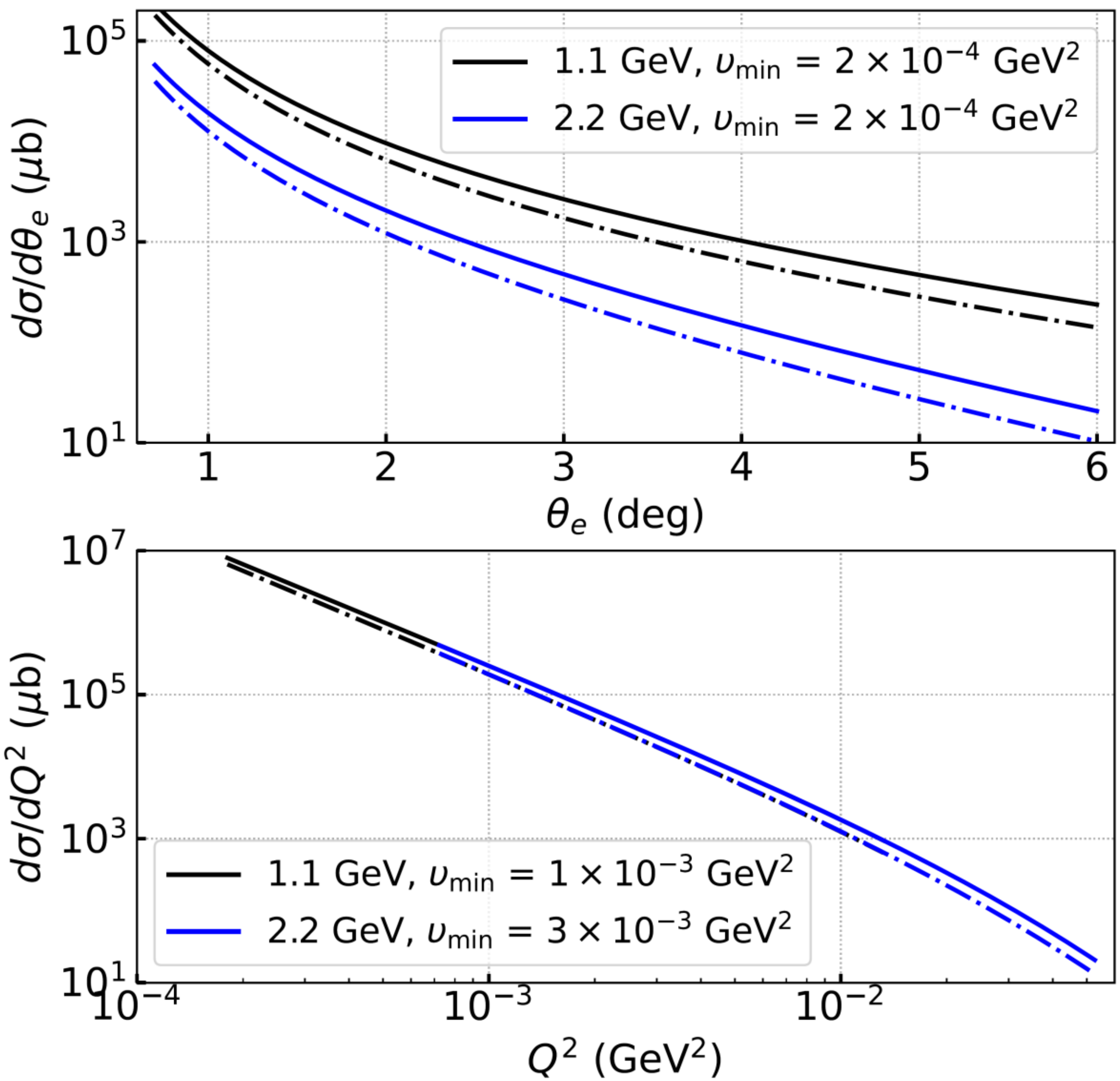

4) Numerical results

(Top panel)

<u>Unpolarized elastic **e-d** scattering</u>
Radiative correction $\boldsymbol{\delta_{ed}}$ as a function of Q^2 for different values of inelasticity cut and at
E_1 = 1.1 GeV (solid lines),
E_1 = 2.2 GeV (dashed lines)

(Bottom panel)

Møller <u>scattering</u>
Radiative correction $\boldsymbol{\delta_{ee}}$ as a function of Q^2 for different values of inelasticity cut and at
E_1 = 1.1 GeV (solid lines),
E_1 = 2.2 GeV (dashed lines)

Abbott1 form-factor model used in calculations of $\boldsymbol{\delta_{ed}}$ curves

Values of $\boldsymbol{v_{min}}$ and $\boldsymbol{Q^2}$ chosen according to kinematics coverage of DRad experiment for each process

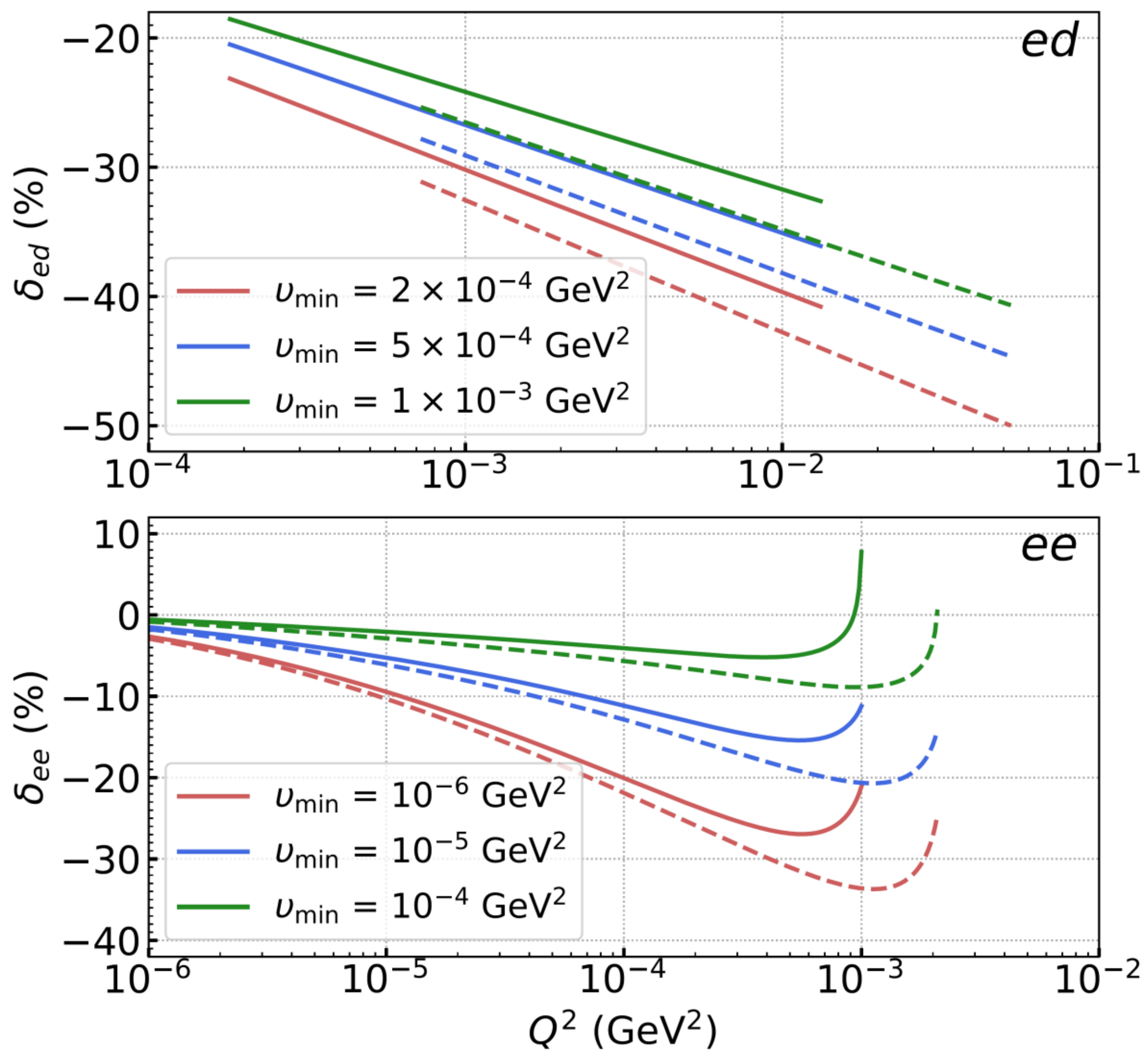

4) Numerical results

(Top panel)

<u>Unpolarized elastic **e-p** scattering</u>
Radiative correction $\boldsymbol{\delta_{ep}}$ as a function of Q^2 for different values of inelasticity cut and at
E_1 = 1.1 GeV (solid lines),
E_1 = 2.2 GeV (dashed lines)

(Bottom panel)

Møller <u>scattering</u>
Radiative correction $\boldsymbol{\delta_{ee}}$ as a function of Q^2 for different values of inelasticity cut and at
E_1 = 1.1 GeV (solid lines),
E_1 = 2.2 GeV (dashed lines)

This figure is from epja1

Radiative corrections for PRad studies

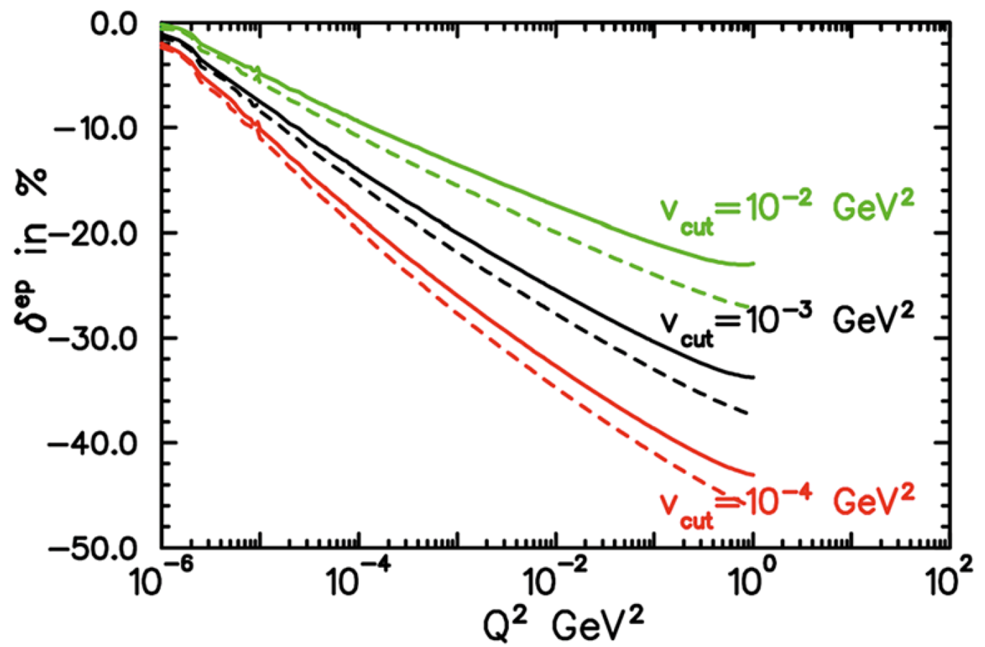

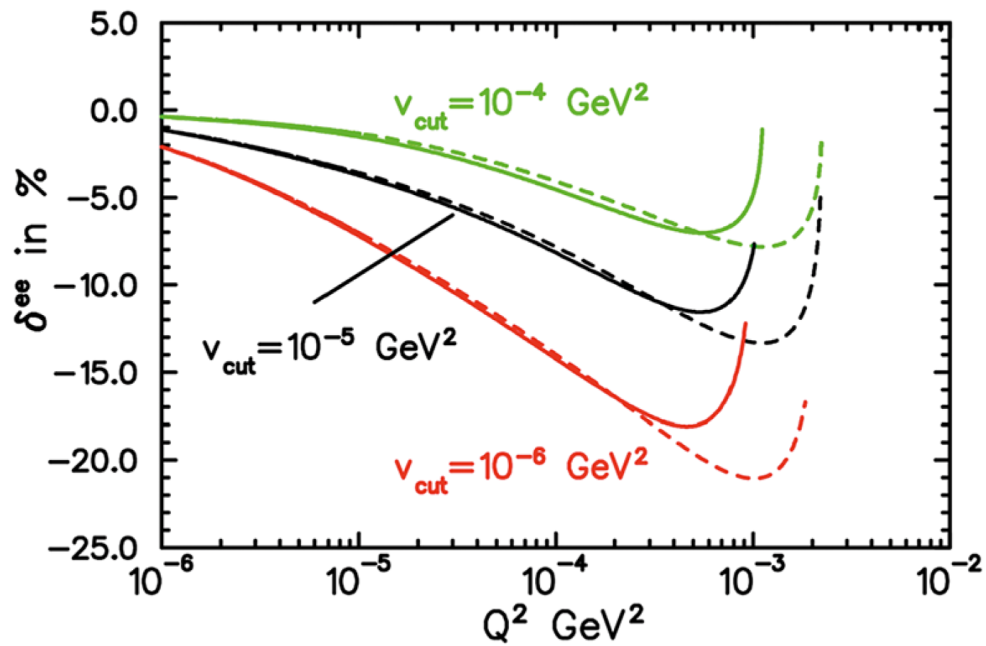

4) Numerical results

(Top panel)

Relative difference of cross sections $d\sigma_{2,3,4}$ between Abbott2, Parker and SOG form-factor models

and

the cross section $d\sigma_1$ of the Abbott1 model

(Bottom panel)

Residual of δ_{ed} between the other form-factor models, $\delta_{ed}^{2,3,4}$,

and

the Abbott1 model, δ_{ed}^{1}

Applied v_{min} is 2×10^{-4} GeV^{-2}

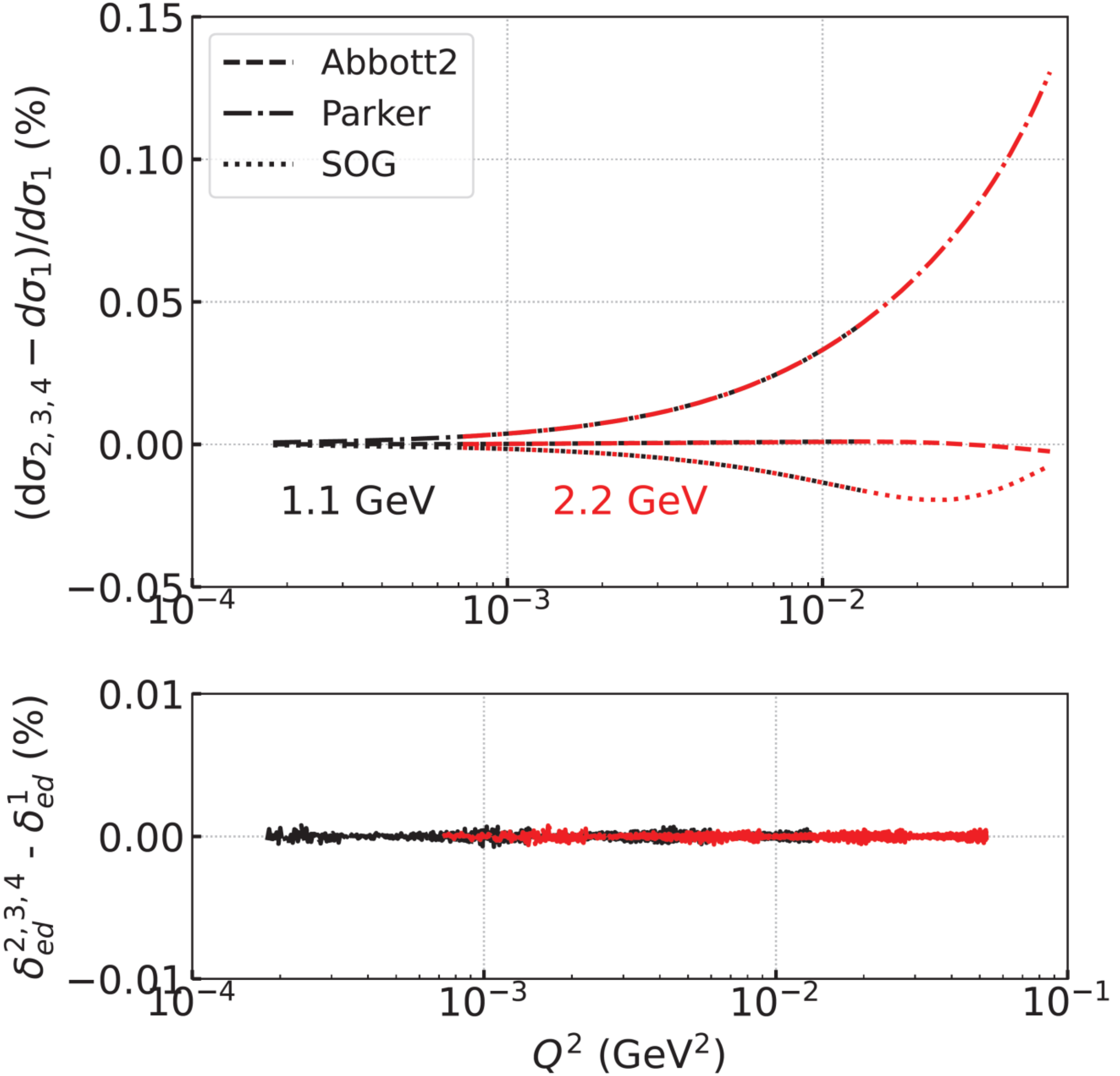

4) Numerical results

<u>Unpolarized elastic **e-d** and **e-p** scattering</u>

Cross sections as a function of scattering angle θ_e:

at

E_1 = 1.1 GeV (top panel)

and

E_1 = 2.2 GeV (bottom panel)

Solid curves showing Born cross section and dot-dashed curves showing total cross sections including RC contributions

Abbott1 form-factor model used in calculations of cross-section curves

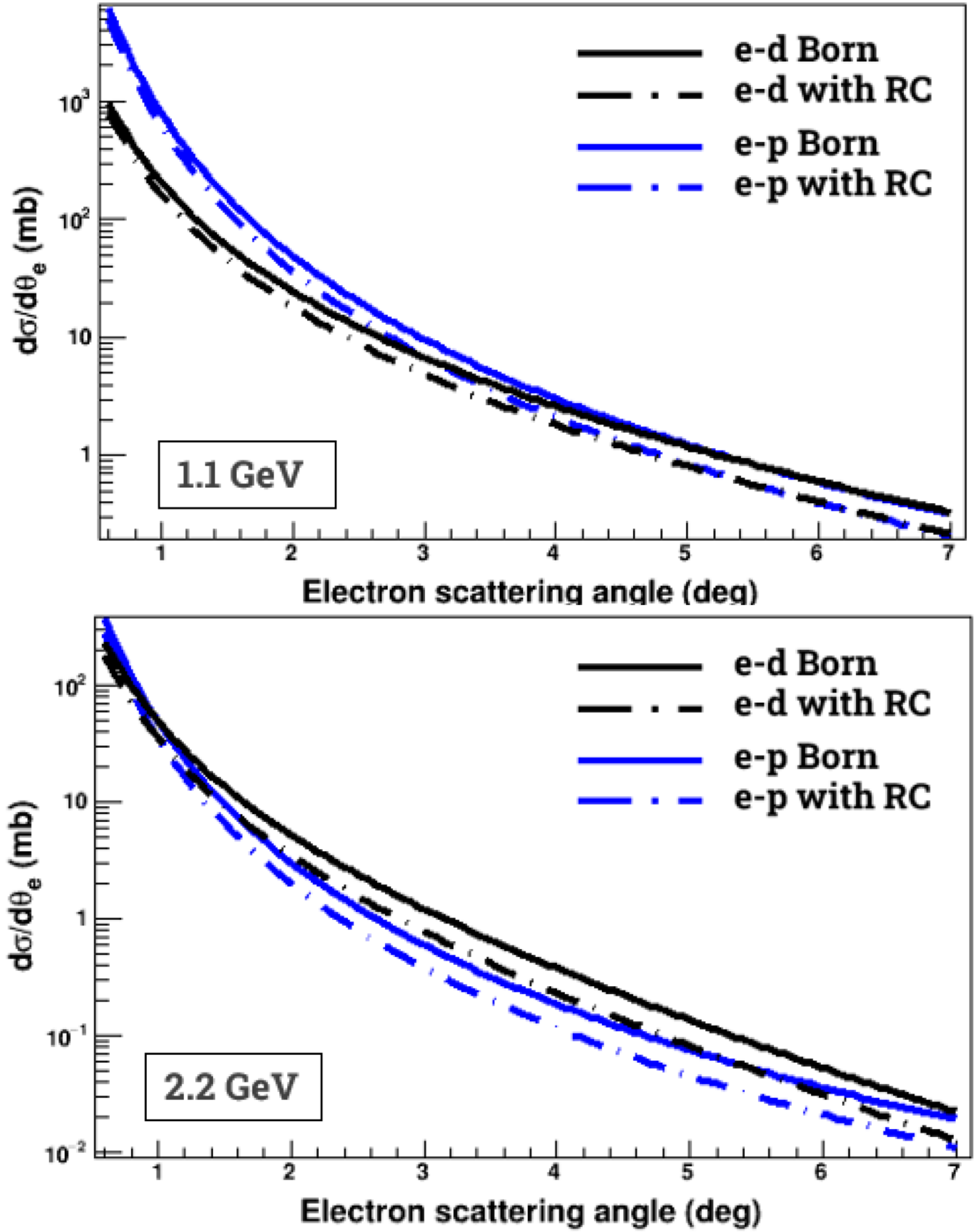

4) Numerical results

- QED RC corrections to elastic e−p scattering at low energies studied

  by Arbuzov and Kopylova, in Eur. Phys. J. C **75,** (2015)

- Same method used by PRad for estimating higher-order RC systematic uncertainty on measured proton radius r_p
  - For e-p RC $\rightarrow$ δr_p = *0.0020* fm; for Møller RC $\rightarrow$ δr_p = 0.0065 fm
  - For total RC $\rightarrow$ δr_p = *0.0069* fm
  - Measured radius in Nature 575, 147 (2019)
    - $r_p = (0.831 \pm 0.007_{\text{stat}} \pm 0.012_{\text{syst}})$ fm

- Using same method for estimating higher-order RC relative systematic uncertainty on deuteron radius r_d
  - 0.06% ~ 0.10% at E_1 = 1.1 GeV beam energy
  - 0.10% ~ 0.15% at E_1 = 2.2 GeV beam energy

5) Proton/deuteron charge radius puzzle

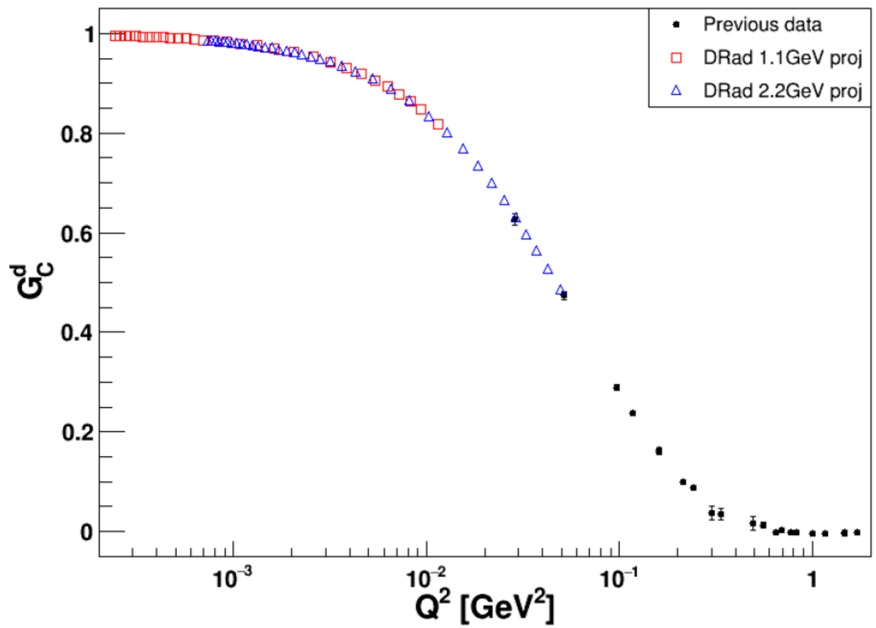

Projected charge form factor of the deuteron over low Q^2 range to be covered in DRad experiment

Also, the shown are previous data at low Q^2

Item	Uncertainty (%)
Event selection	0.110
Radiative correction	0.090
HyCal response	0.043
Geometric acceptance	0.022
Beam energy	0.008
Total correlated terms	0.13

Projected relative uncertainties on the deuteron radius

Item	Uncertainty (%)
Statistical uncertainty	0.05
Total correlated terms	0.13
GEM efficiency	0.03
Inelastic e-d process	0.024
Efficiency of recoil detector	0.15
Total	0.21

Projected total relative uncertainty on the deuteron radius

5) Proton/deuteron charge radius puzzle

- **Proton charge radius puzzle developed and quickly became widely known after 2010**
- Three types of measurements responsible for its origin
  - First r_p determination in 2010 and 2013 by CREMA Collaboration based on muonic hydrogen spectroscopic method by measuring transition between $2S_{1/2}$ & $2P_{3/2}$ energy levels
  - Ordinary atomic hydrogen spectroscopic r_p measurements already compiled by CODATA-2010 (CODATA standing for Committee on Data for Science and Technology)
  - Two values of r_p reported at around same time by electron scattering community

Proton charge radius puzzle

Discrepancy seen in data from

muonic hydrogen spectroscopy

and

ordinary atomic hydrogen spectroscopy plus e-p scattering experiments

Figure credit:
Paul Scherrer Institut

https://www.psi.ch/en/muonic-atoms

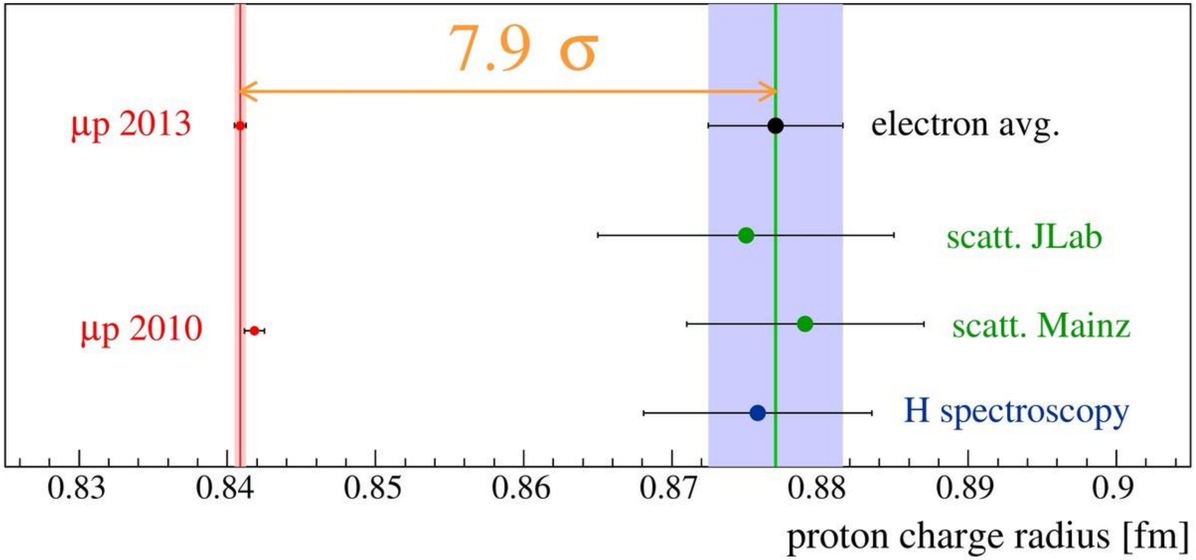

5) Proton/deuteron charge radius puzzle

➢ However, currently “smaller” puzzles exist within the main puzzle

- First, between various ordinary atomic hydrogen spectroscopic measurements

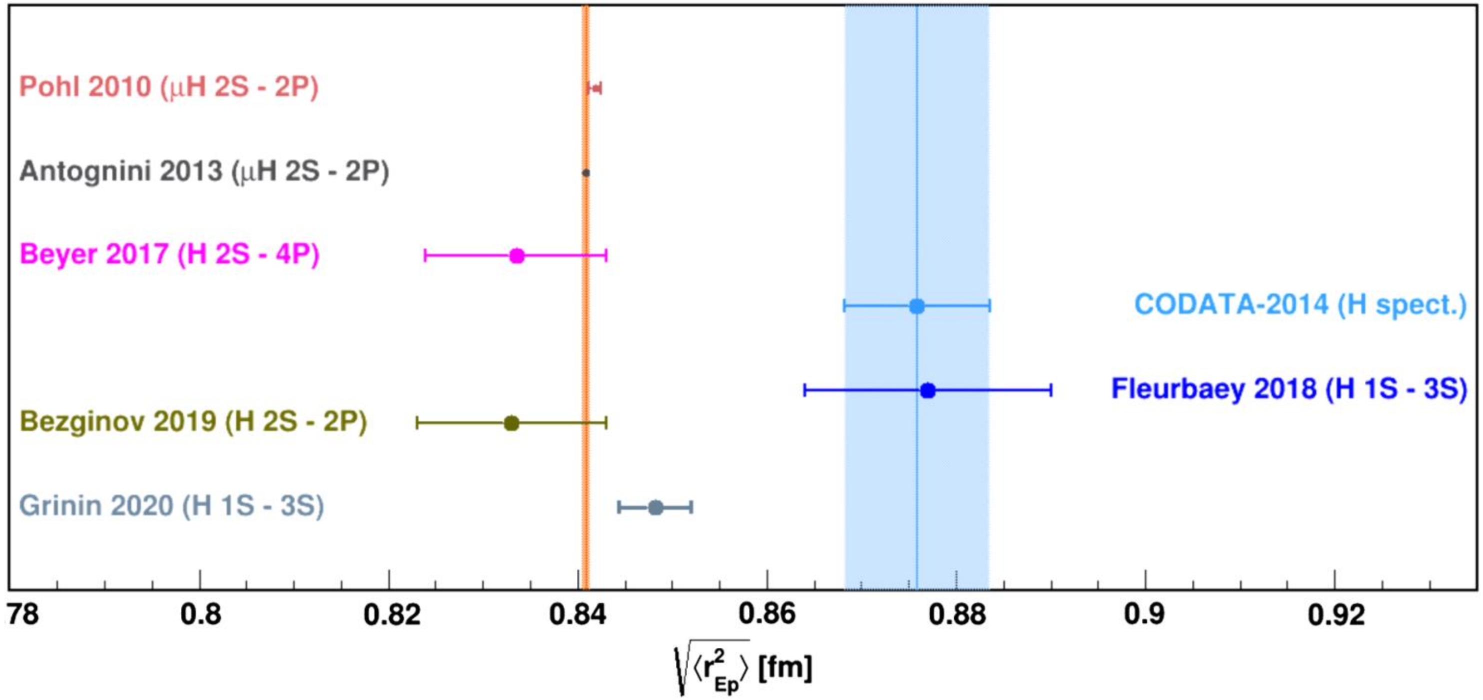

Latest r_p results from

various atomic hydrogen spectroscopic measurements

along with CODATA-2014 recommended value based on ordinary hydrogen spectroscopy

Figure credit: Jingyi Zhou

5) Proton/deuteron charge radius puzzle

➢ However, currently “smaller” puzzles exist within the main puzzle

- Second, between various e-p scattering experiments

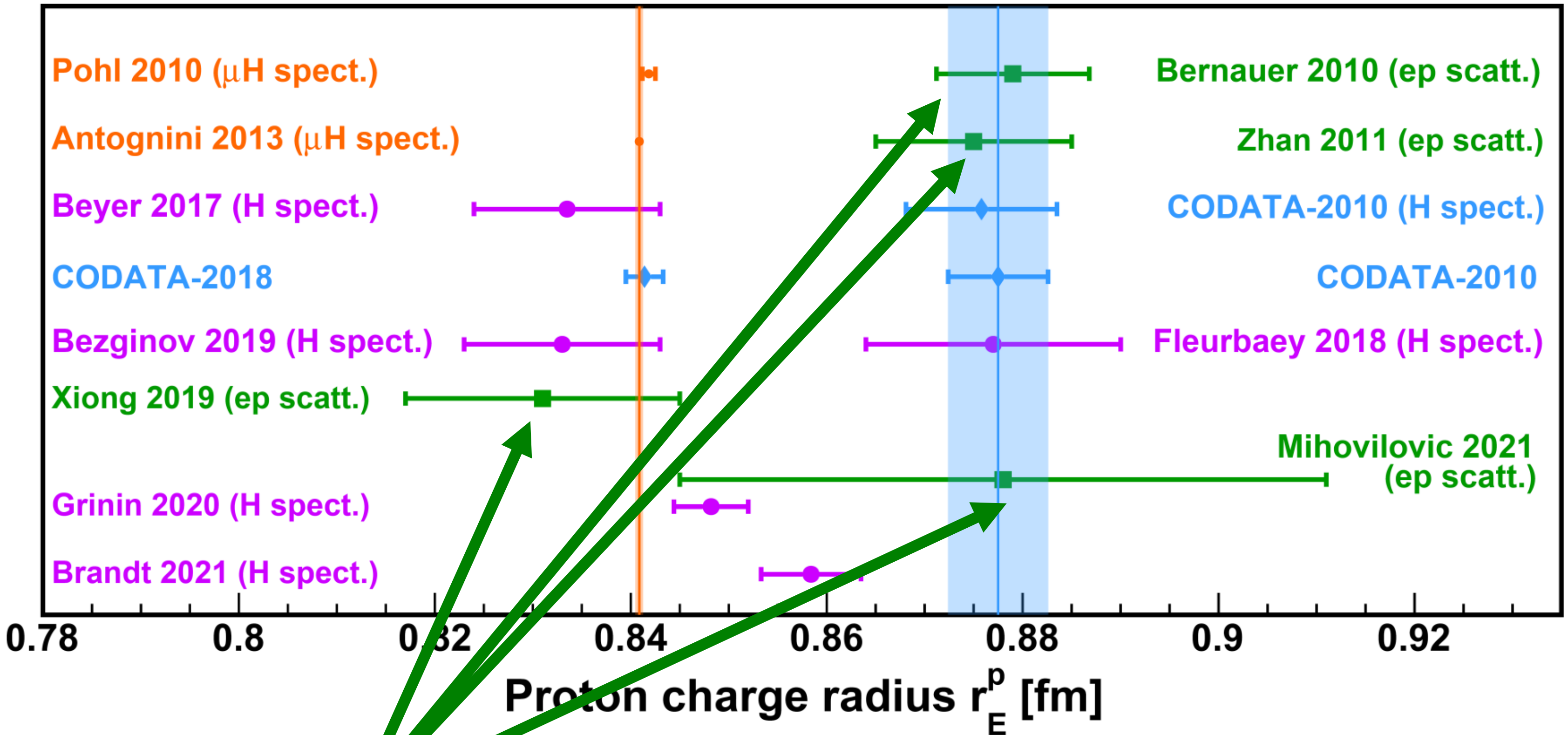

Latest r_p results from various e-p scattering experiments

Figure credit: Jingyi Zhou

5) Proton/deuteron charge radius puzzle

➢ Whole proton charge radius puzzle include discrepancies among

- muonic H and atomic H spectroscopic measurements
- muonic H spectroscopic measurements and e-p scattering experiments
- atomic H spectroscopic measurements and e-p scattering experiments
- various atomic H measurements
- various e-p scattering experiments

Additional r_p results are shown from

various re-analyses of e-p scattering data, including global fits carried out after 2010

Figure credit: Jingyi Zhou

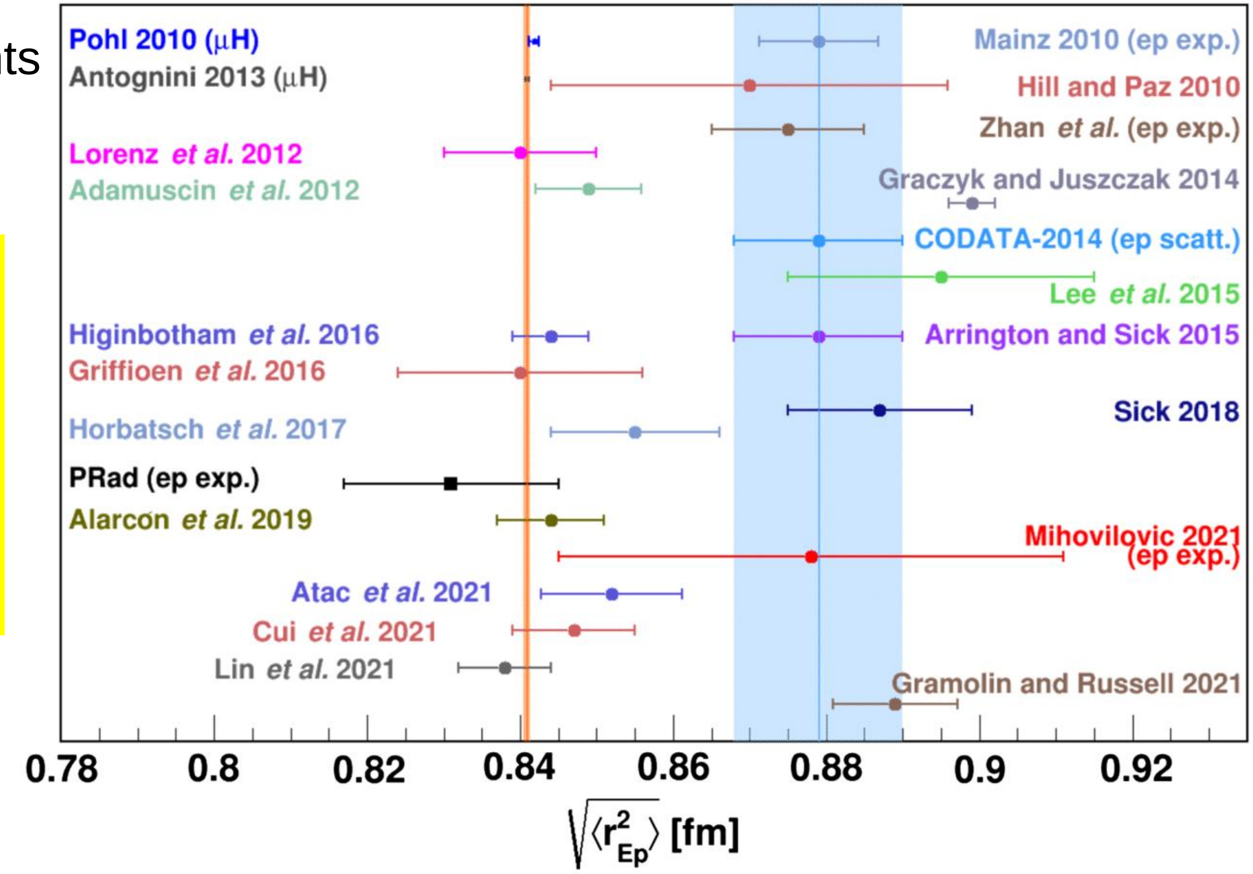

5) Proton/deuteron charge radius puzzle

Latest r_p results from lattice QCD calculations

compared to muonic H measurement

and CODATA-2014 recommended value determined from e-p scattering

Figure credit: Weizhi Xiong

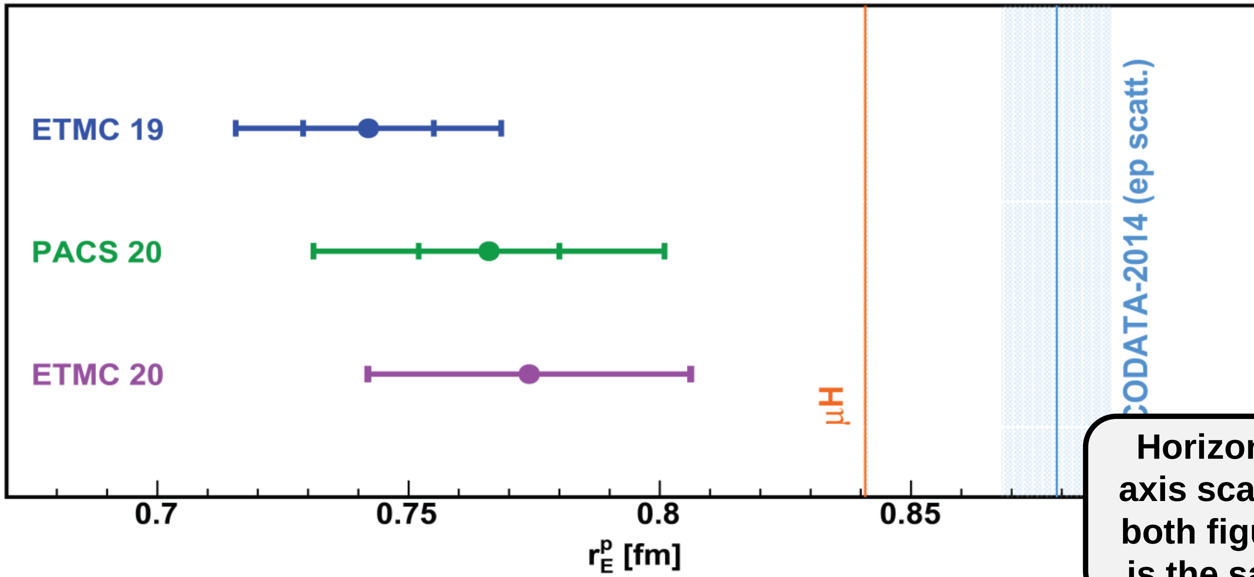

Horizontal axis scale in both figures is the same

- Entire picture becomes more puzzling after including lattice QCD radius results

Other r_p results are shown by black color points obtained from re-analyses of e-p scattering data

e-p scattering data are shown by green, red, and blue colors

Figure credit: Weizhi Xiong

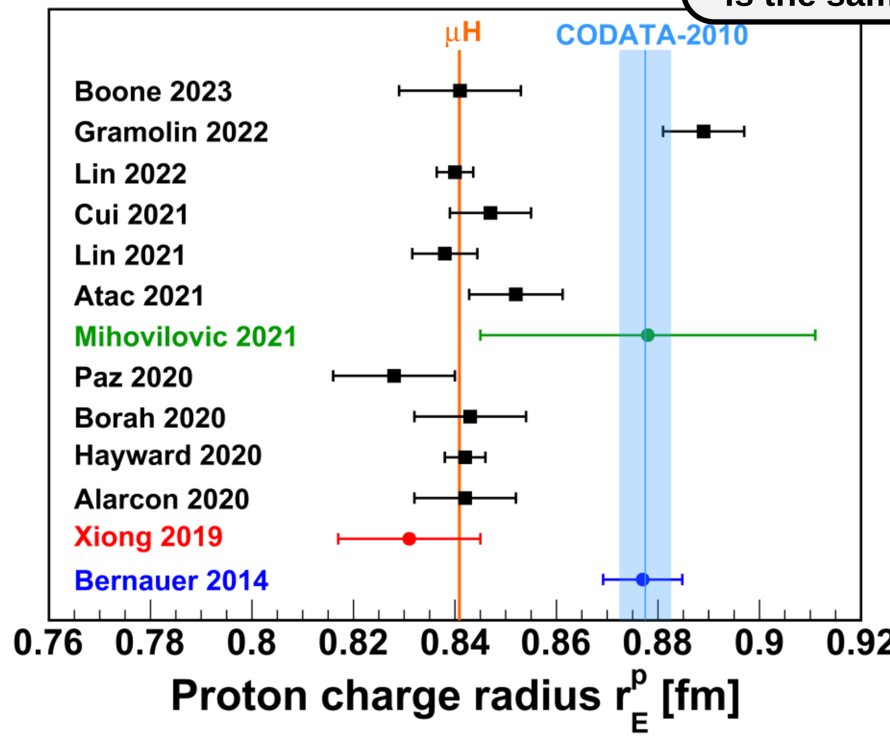

5) Proton/deuteron charge radius puzzle

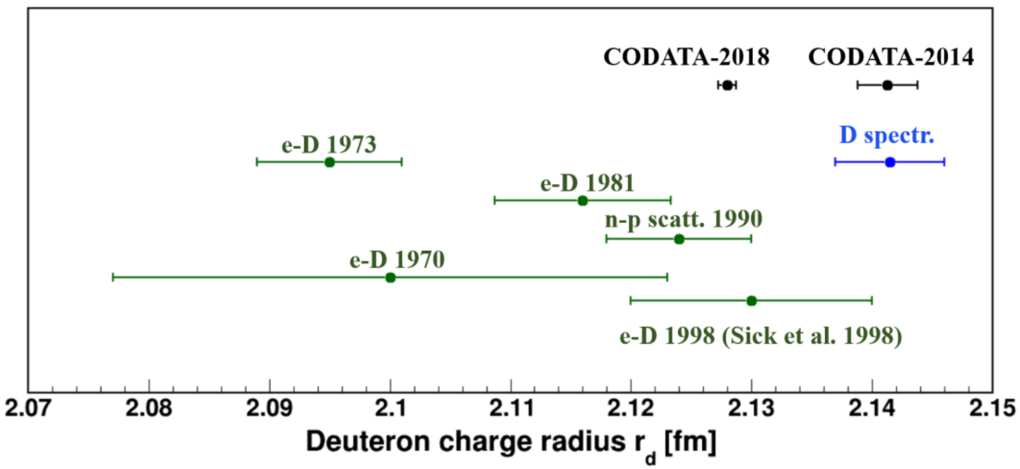

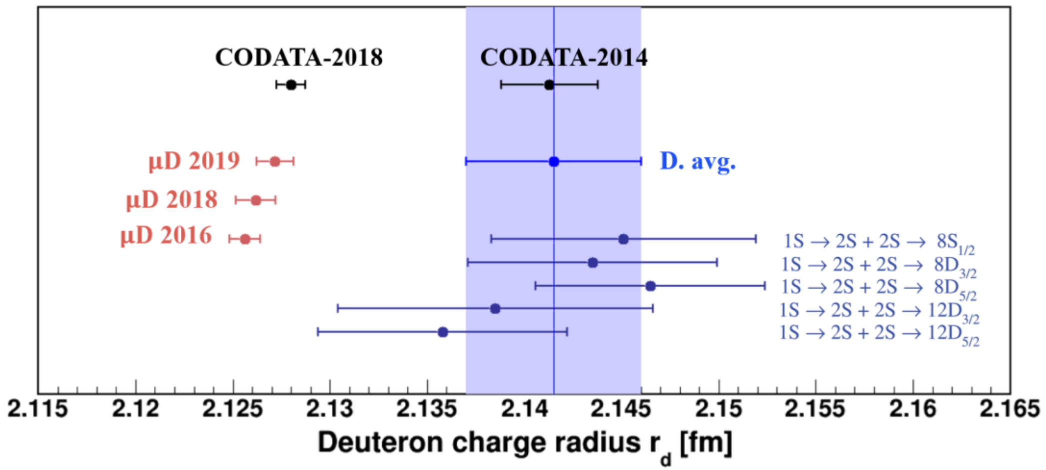

Existing data from e-d scattering and n-p scattering

CODATA values shown along with existing data from atomic and muonic deuterium spectroscopy

CODATA values shown along with all data from e-d scattering, atomic and muonic deuterium spectroscopy

Figure credit: Randolf Pohl

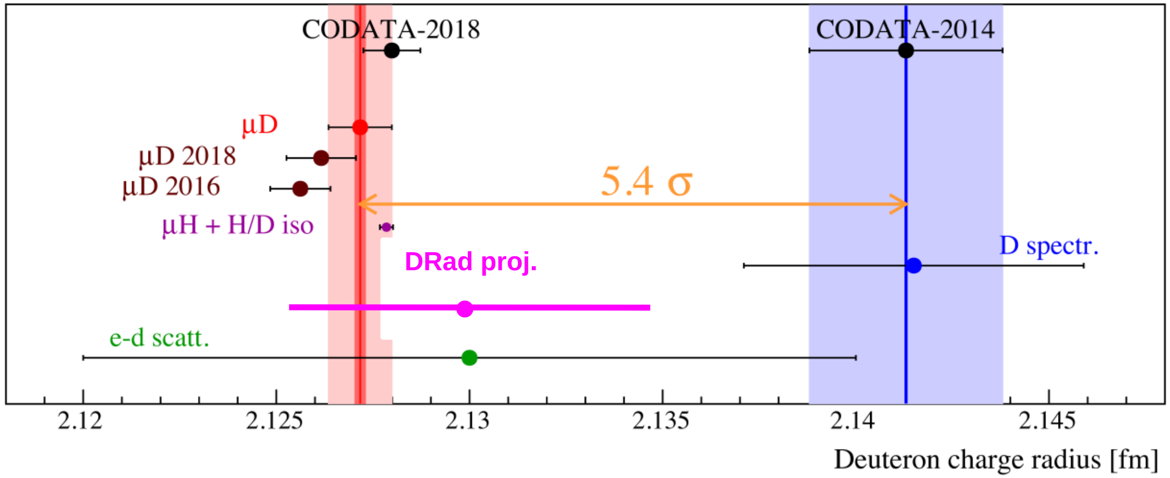

Summary

- We discussed lowest-order radiative corrections in unpolarized elastic e+d scattering

- Some numerical results shown for the proposed DRad experiment at Jefferson Lab
  - Project deuteron charge form factor now
  - Extract deuteron radius from data later

- We discussed proton and deuteron charge radius puzzles

Thanks !

Backups

Additional information on proton charge radius puzzle

PRad-II projection for r_p

shown with a few selected results from other experiments and CODATA-2018 recommendation

Figure credit: Jingyi Zhou

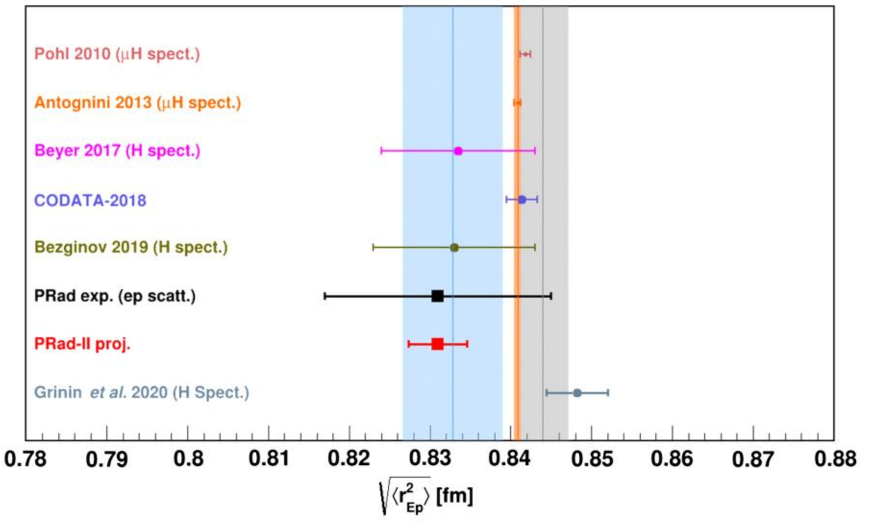

Horizontal axis scale in both figures is the same

Similar as above

with more data shown

with more CODATA recommendations shown

Figure is from PRad-II proposal arXiv:2009.10510 [nucl-ex]

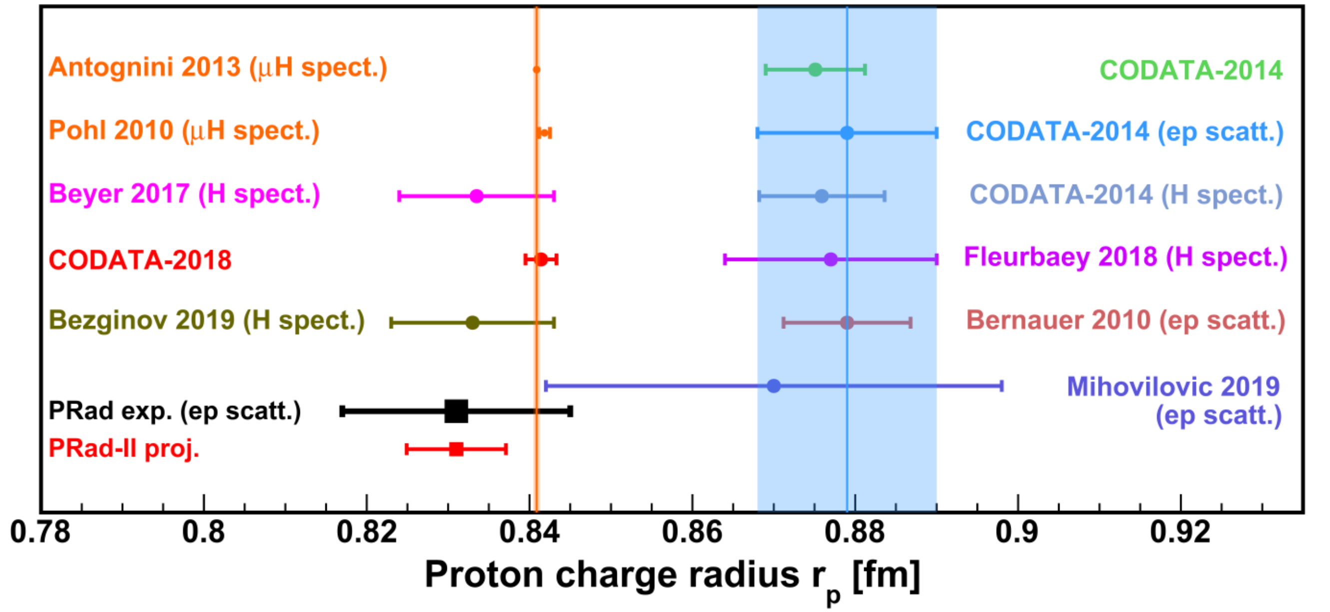

Additional information on Introduction

- PRad collaboration proposed measurements of e-d elastic scattering to also provide new result on deuteron charge radius r_d
  - with a planned experiment called DRad
  - with kinematic coverage of Q^2 from 1.8×10^{-4} $(\mathrm{GeV/c})^2$ to 5.3×10^{-2} $(\mathrm{GeV/c})^2$
  - with two electron beam energies 1.1 GeV and 2.2 GeV

- DRad aiming at overall relative precision of 0.22% (or better) in determination of r_d

- Note that last time elastic e-d cross-section measurement was carried out several years ago
  - by A1 collaboration at Mainz Microtron, with its data analysis currently ongoing
  - however, unpublished PhD thesis reports $r_d = 2.121 \pm 0.007 \pm 0.014$ fm

- Determine deuteron charge radius from elastic e-d structure function slope

$$r_d^2 = -6\left[\frac{dA(Q^2)}{dQ^2}\right]_{Q^2=0}$$

PRad and PRad II systematic uncertainties

Item	PRad δr_p [fm]	PRad-II δr_p [fm]	Result
Stat. uncertainty	0.0075	0.0017	More beam time and higher DAQ rate
GEM efficiency	0.0042	0.0008	2nd tracking detector
Acceptance	0.0026	0.0002	2nd tracking detector
Beam energy related	0.0022	0.0002	2nd tracking detector
Event selection	0.0070	0.0027	2nd tracking + HyCal upgrade
HyCal response	0.0029	Negligible	HyCal upgrade
Beam background	0.0039	0.0016	Better vacuum 2nd halo blocker vertex res. (2nd tracking)
Radiative correction	0.0069	0.0004	Improved calc.
Inelastic ep	0.0009	Negligible	Upgraded HyCal
G_M^p parameterization	0.0006	0.0005	---
Total syst. uncertainty	0.0115	0.0032	
Total uncertainty	**0.0137**	**0.0036**	

PRad systematic uncertainties

Item	r_p uncertainty (fm)
Event selection	0.0070
Radiative correction	0.0069
Detector efficiency	0.0042
Beam background	0.0039
HyCal response	0.0029
Acceptance	0.0026
Beam energy	0.0022
Inelastic ep	0.0009
Total	0.0116

Different uncertainty contributions to the proton radius total uncertainty are given in term of fm

The measured radius is
$r_p = (0.831 \pm 0.007_{stat} \pm 0.012_{syst})$ fm

W. Xiong et al., Nature 575, 147 (2019)

Our goal is to exactly calculate this contribution for the PRad-II experiment

For that purpose we should continue the studies of one-loop (NLO) and two-loop (NNLO) radiative corrections from the Møller scattering

Additional information on Møller scattering

- For the e+p scattering the complete cross section is given by

$$\sigma = \sigma_0 \left(1 + \frac{\alpha}{\pi}(\delta_{VR} + \delta_{\rm vac} - \delta_{\rm inf})\right) e^{\frac{\alpha}{\pi}\delta_{\rm inf}} + \sigma_{\rm AMM} + \sigma_F,$$

where σ_0 is the Born cross section, σ_{AMM} - the anomalous magnetic moment and σ_F - the infrared divergence free contributions to the cross section

δ_{VR} is the infrared divergent contribution, δ_{vac} is the vacuum polarization contribution, δ_{inf} term is to account for multi-photon emission at $Q^2 \to 0$

- For the Møller scattering the complete cross section is given by

$$\sigma^{ee} = \left(1 + \frac{\alpha}{\pi}\left(J_0 \log\frac{v_{\rm max}}{m^2} + \delta_1^H + \delta_1^S\right)\right)\sigma_0 + \sigma_S + \sigma_{\rm vert}^F + \sigma_B^F + \sigma_F,$$

where the infrared divergent contribution of bremsstrahlung is represented as a sum of three factorized corrections

$$\sigma_{IR} = \frac{\alpha}{\pi}\left(J_0 \log\frac{v_{\rm max}}{m\lambda} + \delta_1^H + \delta_1^S\right)\sigma_0$$

from **epja1**

Additional information on numerical results

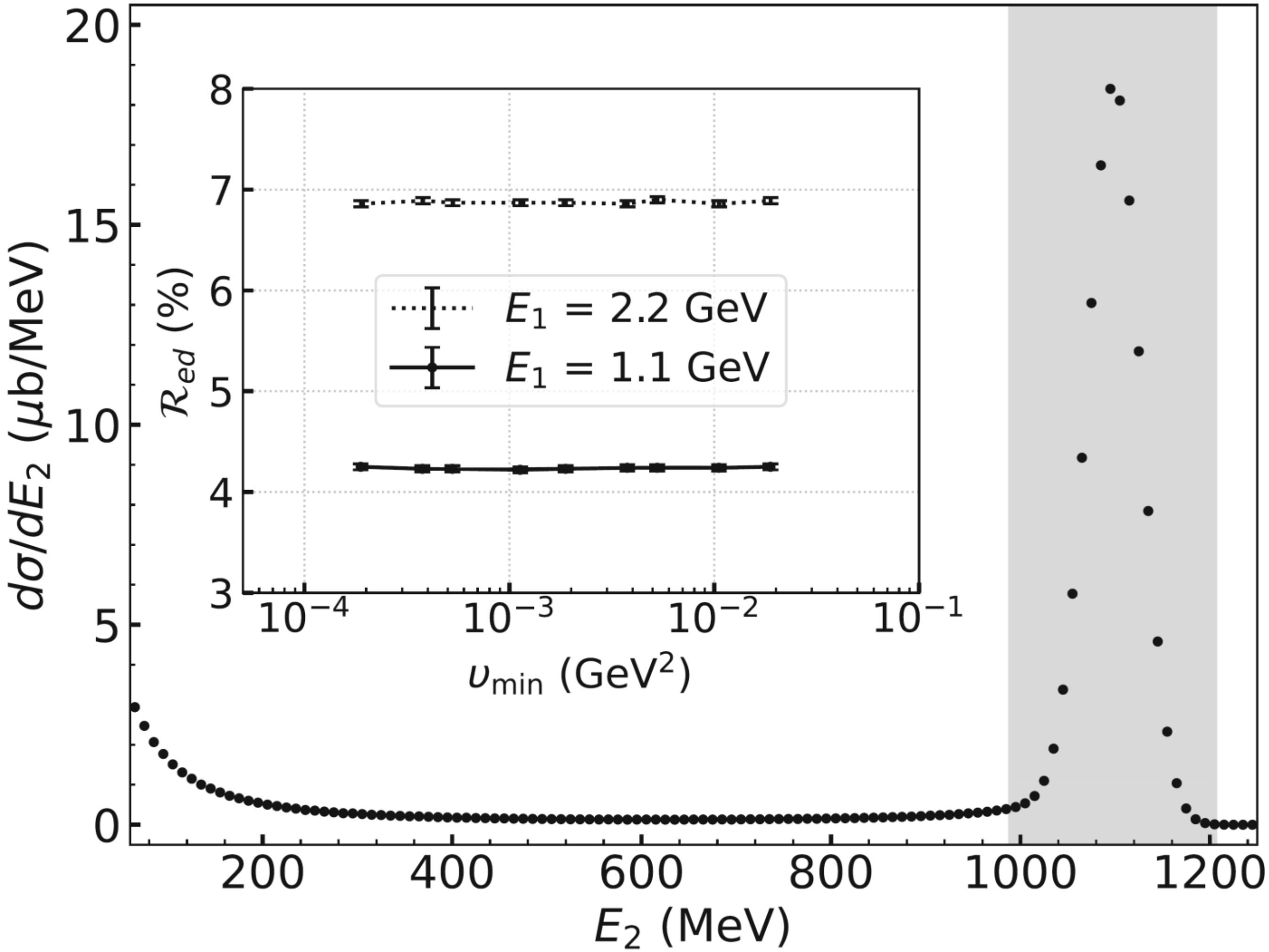

$\mathcal{R}_{ed} =$

$= (\sigma^{obs}/\sigma^{B}) - 1$

R_{ed} showing relative difference between observed and Born cross sections integrated over DRad acceptance and within energy (elasticity) cut

Normalized distribution of e−d events with hard radiative photons simulated by the DRad generator at 1.1GeV

Inset showing R_{ed} as a function of υ_{min} within the range of Q^2 from 2.0×10^{-4} $(\mathrm{GeV/c})^2$ to 2.0×10^{-2} $(\mathrm{GeV/c})^2$

R_{ed} is very stable being 4.2% at 1.1 GeV and 6.9% at 2.2 GeV